

Backgrounds at future linear colliders

Oleg Markin*

Institute for Theoretical and Experimental Physics, Moscow

Abstract

A brief review of the background for experiments at future e^+e^- linear colliders is done. Two sources of background are discussed: the beam delivery system and the interaction point. The abundance of background muons, neutrons, photons and e^+e^- pairs is quoted for different sub-detectors and both background sources. The background caused by the beamstrahlung is described in more detail. Space distributions are sketched and the impact on calorimeters is discussed for the background neutrons.

1. Introduction

The background expected in experiments at future e^+e^- linear colliders substantially differs from that was at the LEP because of higher energy and much more narrow beam. Hits caused by background particles seriously complicate the event reconstruction. The negative influence of the backgrounds on energy reconstruction comprises both worse pattern recognition and pile-up. Therefore the presence of the background should be carefully taken into account throughout the computer simulation of benchmark processes. After all, the load of detectors by background signals determines the detector design as well as the choice of technologies for the detecting systems.¹

2. Backgrounds from the beam delivery system

For the purpose of collimating both e^+ and e^- beams of the International Linear Collider (ILC), three metallic primary collimators will be situated at each side from the Interaction Point (IP). There are also protective masks in the beam tunnel. These elements serve to purify the beam, but as they are placed rather close to IP, the interaction of beam particles with these collimators and masks gives rise to background. The first of the collimators has an aperture $8\sigma_x \times 65\sigma_y$, where σ_x and σ_y are the standard deviations of the transverse density of beam. That collimator is placed about 1,500 m from IP, while two other collimators are about 1,300 m and 1,000 m from IP, respectively.

The presence of the collimators leads to the loss of beam particles, this is shown in fig. 1 for positrons as predicted by two different MC codes. The magnitude of the loss is about 0.1 %; the lost positrons/electrons are being converted to γ s, electron-positron pairs, muon-antimuon pairs and neutrons. These (background) particles contribute to so-called the Beam Delivery System (BDS) background. Besides, the BDS background includes photons originated from bremsstrahlung at gas molecules in the beam tunnel and from the synchrotron radiation. In addition to the BDS background, there is an IP-related background.

*e-mail: markin@itep.ru

¹This review represents studies of background completed to the autumn of 2012.

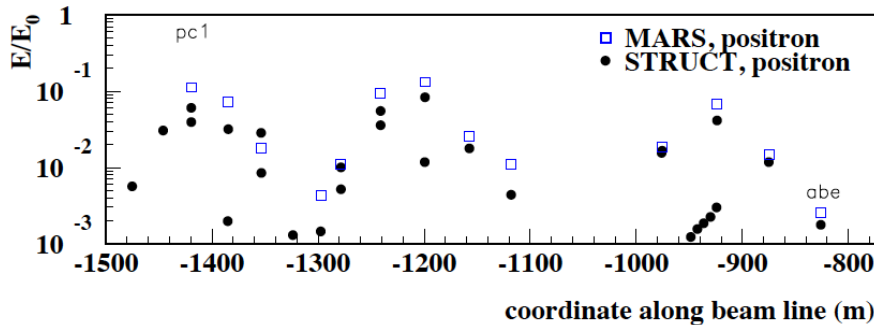


Figure 1. Predictions of two different MC models for the loss of beam energy along the beam line [1].

The BDS neutrons can be created in photo-nuclear reactions. Muons can be produced in electromagnetic showers initiated by beam particles. The probability of the muon production is proportional to the squared charge of nuclei involved in the process, and amounts about $4 \cdot 10^{-4}$ [2]. Thus, the process results in about 4,000 muons for the 0.1% loss of 10^{10} positrons/electrons per bunch-crossing (BX). A good way to minimize the number of those muons is to sweep them away by the magnetic field created by iron spoilers built purposely, cf. fig. 2. There are two possible locations and different constructions of the spoilers: wall- and donut-shape; fig. 3 demonstrates the effect of the two constructions.

The spoilers drastically reduce the muon density, making it several thousand times lower at the entrance to the experimental hall. A side effect of the spoilers is increasing of the number of neutrons, see table in the fig. 4. The neutrons from the BDS background are not a problem since a concrete wall will be placed at the entrance to the experimental hall. The vertex system (VTX) is the only sub-detector not affected by the muon spoilers.

The energy distribution of the BDS muons and neutrons is shown in fig. 5. The BDS muons and neutrons have rather flat radial distribution within three meters from the beam axis, see fig. 5. The BDS photons and positrons/electrons are concentrated near or inside the beam pipe. The BDS background dominates in the muon detector while in the tracker and the VTX it gives the number of hits that does not exceed the IP background [3].

3. Backgrounds related to the interaction point

3.1. Hard photons

At high-energy colliders the electromagnetic field of each bunch causes focusing of bunches of the opposite beam. That leads to bending of electron/positron trajectories near the IP, which results in emission of hard photons. At the ILC, this process (called beamstrahlung) will give about two photons per a beam particle, with the average energy of beamstrahlung photons being several percents of the beam energy [4]. The spectrum of the beamstrahlung photons is shown in fig. 6. The beamstrahlung photons are strongly focused in forward direction and, therefore, do not significantly contribute to the detector background. However, the beamstrahlung photons produce electron-positron pairs that do contribute to the detector background either directly or through their backscatters. The photons can also produce neutrons when they hit components of the beam delivery system, such as collimators and the beamstrahlung dump.

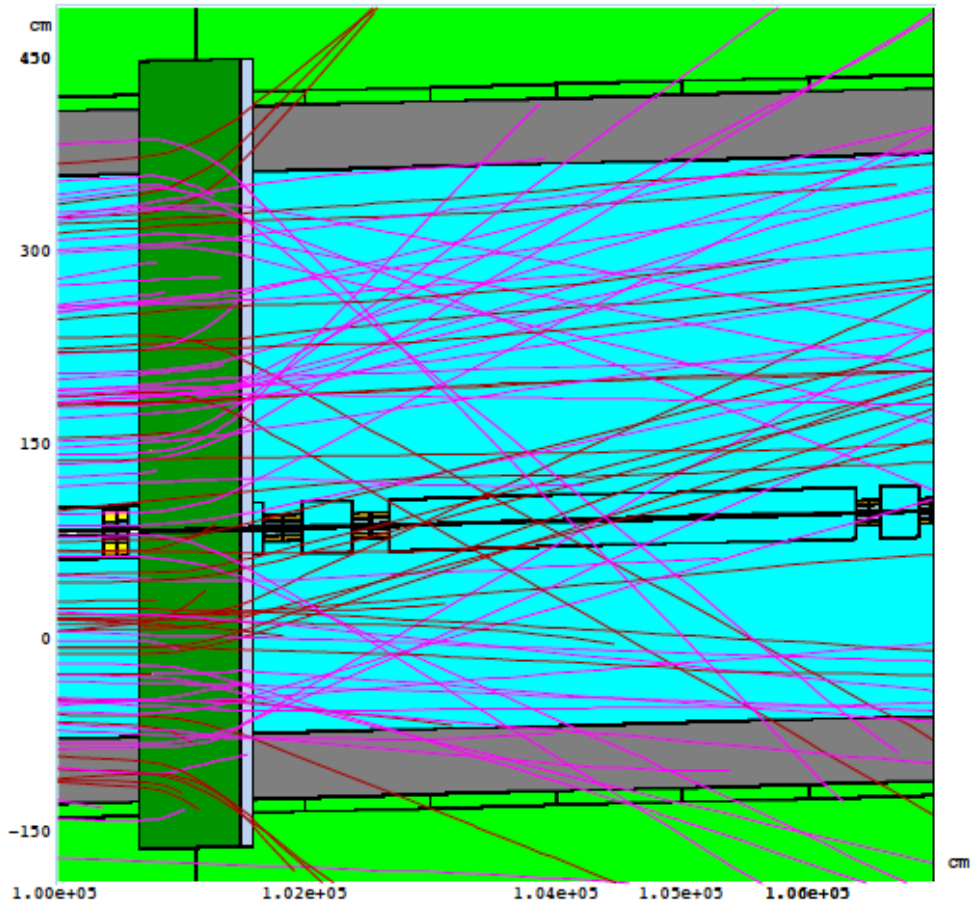


Figure 2. Muon tracks in the spoiler region [3].

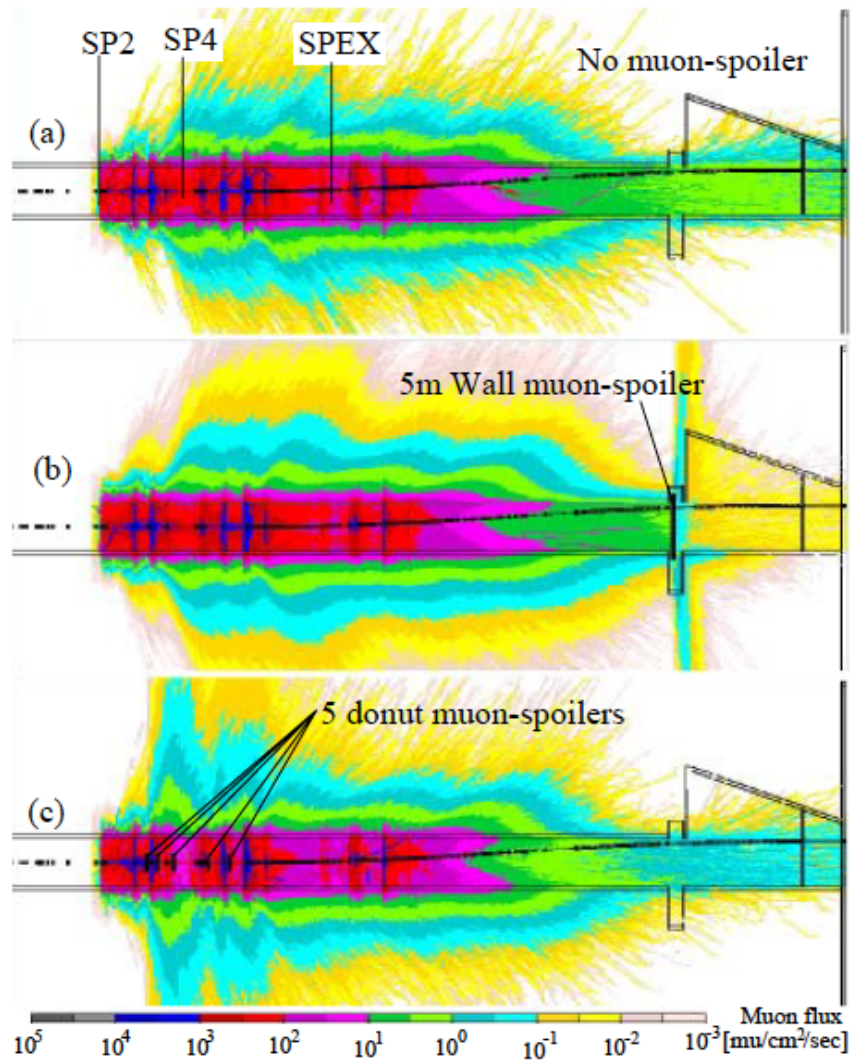


Figure 3. Two-dimensional distributions of total muon flux for (a) no, (b) wall- and (c) donut-shape muon spoilers [1]. The notations SP2, SP2 and SPEX stand for the three primary collimators discussed in the text.

	γ	μ^\pm	e^+	e^-	neutron
With spoilers	2927	0.024	1172	$3.6 \cdot 10^{-4}$	6364
No spoilers	2942	60.4	1095	10	346

Figure 4. Average number of particles per bunch at the beginning of detector from positron tunnel [3].

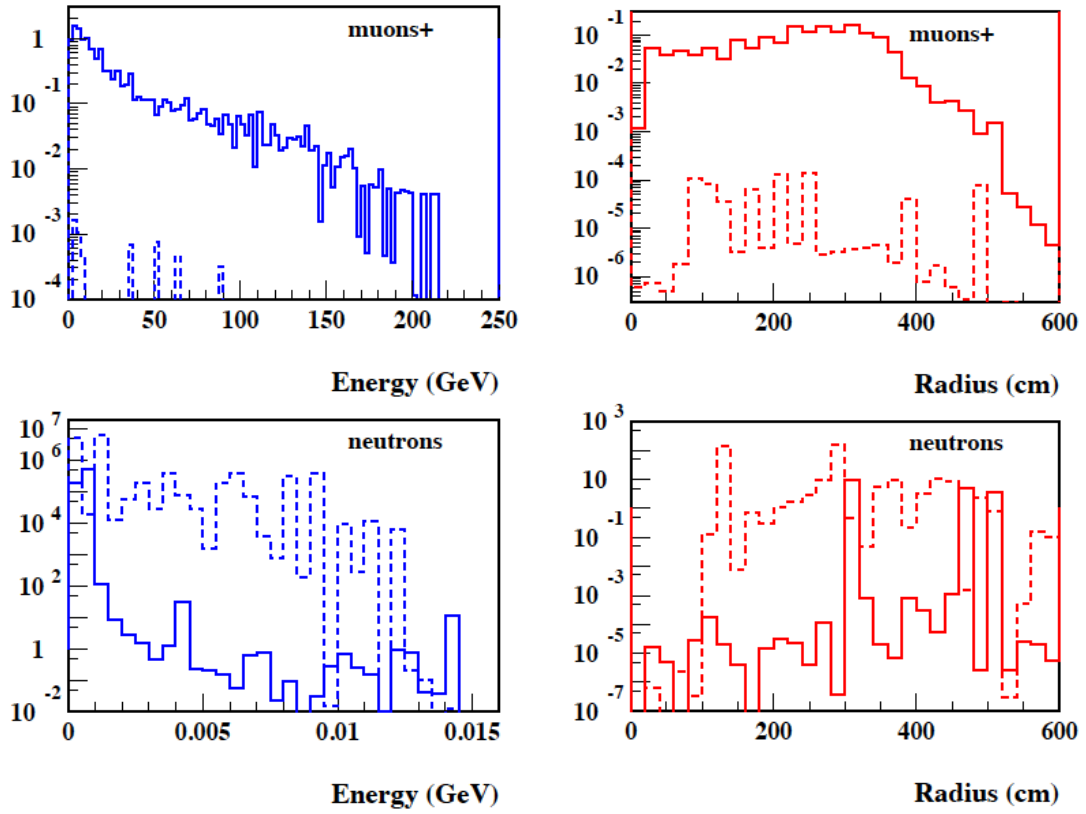


Figure 5. Left: energy spectra of particles at the detector (per bunch); solid line — no spoilers, dashed line — tunnel with spoilers. Right: radial distributions of particles at the detector [3]. Shown are particles coming from positron tunnel only.

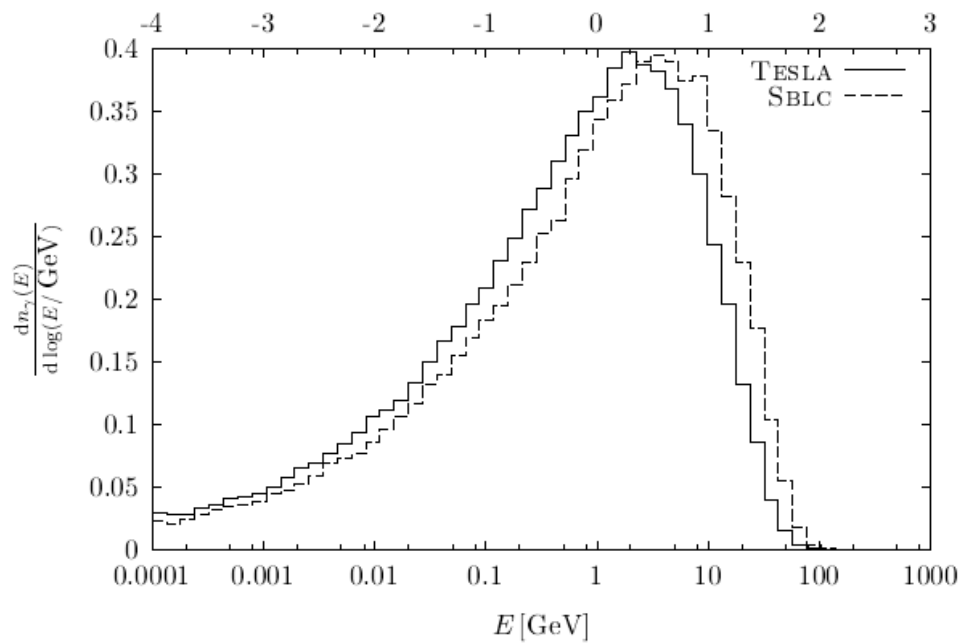


Figure 6. The spectrum of beamstrahlung photons for two ILC-like colliders [4].

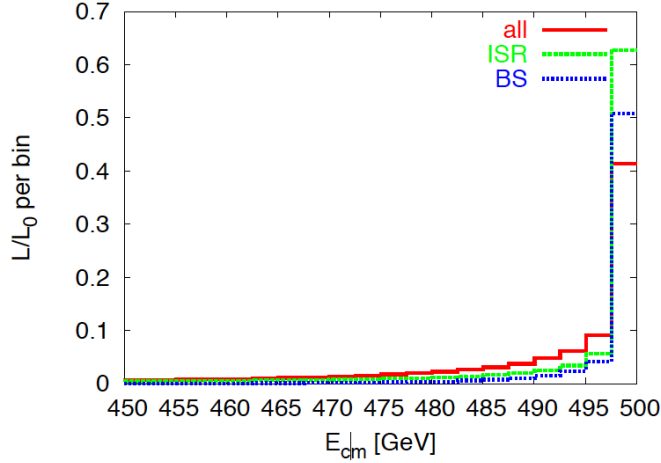


Figure 7. Relative luminosity spectrum, considering beamstrahlung (BS), initial state radiation (ISR) and both (all) [5].

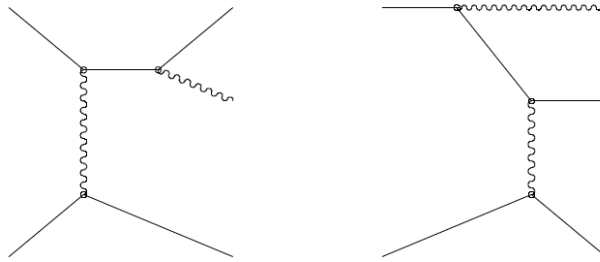


Figure 8. Diagrams of radiative Bhabha scattering.

Besides, hard photons can be created in the ordinary initial state radiation. Both the initial state radiation and the beamstrahlung reduce the luminosity of colliders in the region close to nominal energy, cf. fig. 7. A prominent source of hard photons is the collision of two beam particles resulting in bremsstrahlung, called the radiative Bhabha scattering, see fig. 8. The photons created in the radiative Bhabha scattering are also focused in the forward direction, and escape through the beam pipe, but the remnant electrons/positrons contribute to the detector background.

3.2. Soft electrons/positrons

The basic process that gives rise to the detector background is the creation of electron-positron pairs additional to beam particles. An electron-positron pair can be created by a beamstrahlung photon in the strong electromagnetic field of beams. This is referred to as the coherent pair production. Under conditions of the Compact Linear Collider (CLIC), the newly born pairs constitute several percents of beam particles.

At the ILC, another way of pair creation dominates, which is referred to as the incoherent pair production, when new electron-positron pairs are created as a result of interaction of just two particles. Those can be either two real beamstrahlung photons or a single real beamstrahlung photon plus an electron/positron, or a couple of electrons/positrons, cf. fig. 9. At the ILC with $\sqrt{s} = 0.5$ TeV, there should be about 76,000 pairs per BX, with the average energy 2.5 GeV per an electron/positron [6]. The energy spectrum of the pairs is shown in fig. 10. The interaction of photons can also give a couple of quarks followed by hadronization into minijets.

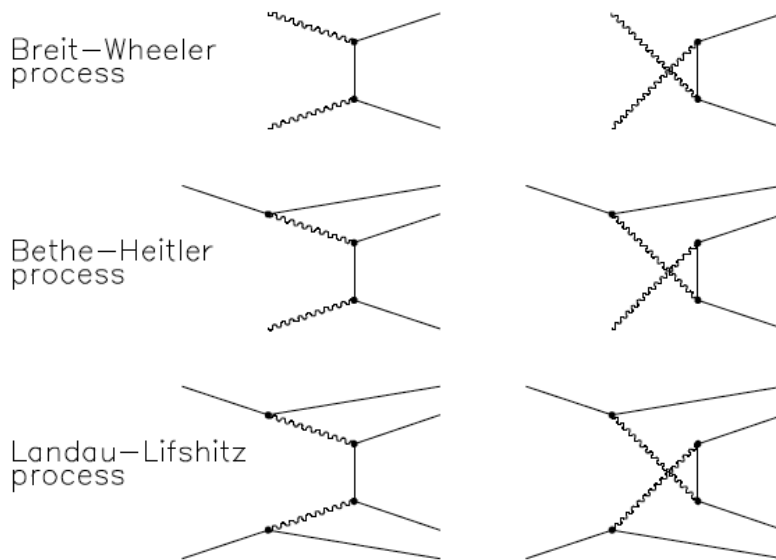


Figure 9. Diagrams of beamstrahlung pairs creation.

An additional to beamstrahlung source of off-energy electrons/positrons is the radiative Bhabha scattering. For that process, the spectrum of remnant beam particles is rather flat at the low energy end [7], see fig. 11. Under the ILC-like conditions, after emission of a photon, the average energy of the scattered electron/positron is equal to 50 GeV on average, and the number of corresponding electron-positron pairs is about $4 \cdot 10^4$ per BX [8].

The electrons/positrons can be either focused or defocused by the beam field, which depends on the absolute value of particle momentum and its direction. The remnant electrons/positrons from radiative Bhabha scattering follow the appropriate beam and are thus focused. They will be dumped inside quadrupole magnets. The electrons/positrons from the beamstrahlung pair production can follow the positive beam direction as well as the negative one, which predetermines focusing [7]. Most of them initially have a small θ -angle with respect to the beam axis. The final angle depends on the deflection by the beam field. The bigger transverse momentum p_t they have, the smaller θ -angle they finally acquire. Therefore, only low- p_t electrons/positrons reach the detector where their range is limited by the main magnetic field, though. For the main part, those electrons/positrons curl up and move longitudinally towards the quadrupoles. They may hit the forward detectors (LumiCal and BeamCal), the mask, the quadrupoles and the beam tube, producing secondaries, photons in that number, which may convert to pairs inside sub-detectors. In the Time Projection Chamber (TPC) for example, the electrons/positrons from the pairs produced by the secondary photons are actually seen as lines (helices with tiny radius) parallel to the field direction [9]. The number of such tracks is about 1,400 per BX, which also includes backscatters from ECal and charged particles from the hadronic reactions in minijets.

3.3. Neutrons

A large amount of electrons/positrons from pairs are deflected by the beam field and can hit the beam pipe and the quadrupole from inside. Thus there are two space origin of the IP-induced background: (i) directly the IP and (ii) backscatters from the beam pipe itself and the very forward region, particularly the BeamCal.

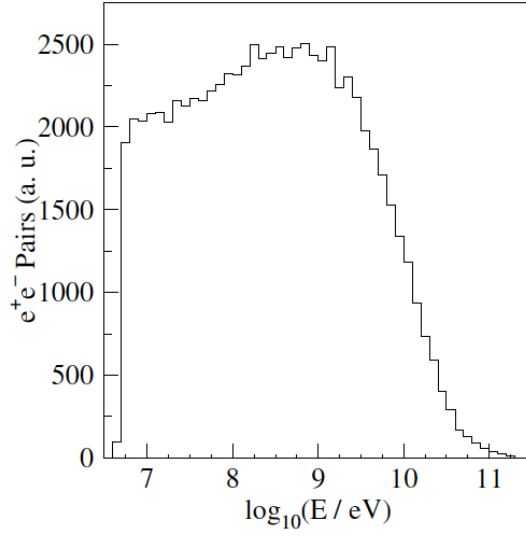


Figure 10. The energy spectrum of electron-positron pairs simulated with GUINEA-PIG. The lower edge at 5 MeV corresponds to a momentum cut-off in the simulation [9].

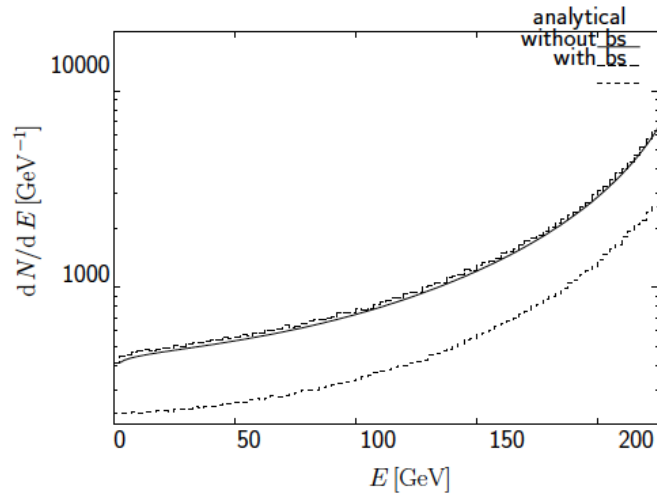


Figure 11. Spectrum of bremsstrahlung photons for an ILC-like collider. The letters 'bs' denote the so-called beam-size effect that almost halves the production rate. The similar reduction occurs for the beamstrahlung pair production rate as well [4].

detector	n from pairs [n/BX]	n from pairs [GeV/BX]	n from RB rad. Bhab. [n/BX]	n from rad. Bhab. [GeV/BX]
ECAL (barrel)	6194	4.69	72	0.009
ECAL (endcap)	2043	1.44	36	0.001
HCAL (barrel)	670	0.87	0	0
HCAL (endcap)	4029	8.03	3792	4.74
LCAL	4880	1.78	0	0
LAT	1642	1.12	0	0
instr. yoke	8429	31.6	54852	121.8
TPC	15070	8.29	132	0.001

Figure 12. The number of neutron hits and their energy deposited (except for TPC) in sub-detectors [8].

The latter serves as an active absorber: it provides shielding of the BDS elements from the incoherent pairs.

Neutrons are produced by photons and electrons/positrons that create electromagnetic showers where a photo-nuclear reaction may take place with a resonance at the photon energy about 10 GeV. For an ILC-like collider, the pairs created by beamstrahlung photons produce about 70,000 neutrons per BX when they hit the mask and quadrupoles [8]. The remnant electrons/positrons from radiative Bhabha scattering produce even more, about $3 \cdot 10^5$ neutrons per BX. Fortunately, they do not reach most of sub-detectors since they are produced at larger distance from IP, cf. the table in fig. 12.

The neutrons created by the incoherent pairs at the BeamCal dominate the background in the endcaps of the Hadronic Calorimeter (HCal). The level of this background is illustrated in fig. 13. For the CLIC beam parameters (presumably at 3 GeV), the line corresponding to the background from incoherent pairs in the right plot in fig. 14 actually represents the neutrons. The cell occupancy in the HCal endcaps at 40 cm from the beam axis is very high, $\mathcal{O}(10^{-2})$ hits per BX, steeply dropping outward. In the ECal endcaps, the dominating contribution to cell occupancy is concerned with the minijet background. It decreases with a radial distance from the beam axis (i.e. with the polar angle of a final-state particle) not as fast as the neutron background in the HCal endcaps, cf. the left plot in fig. 14.

The signal of clusters created by particles from minijets can be rejected making use of precise time stamping. That has been studied throughout the preparation of the CLIC CDR by including the background from $\gamma\gamma \rightarrow$ hadrons to simulation of several benchmark processes. For neutrons such a rejection procedure based on the time stamp might be less effective. Moreover, the substantial difference exists between the neutron background and the backgrounds from pairs or $\gamma\gamma \rightarrow$ hadrons since neutrons can deposit their energy through low-energy recoil protons in scintillator, which can produce ionization signals much exceeding those of MIP, amplifying thus the calorimeter response to the neutrons. Still, the background from neutrons created by the incoherent pairs could have a significant impact on the reconstruction of events only at very small polar angles because of the steep radial dependence, cf. fig. 14.

Neutrons are also abundantly produced in water and concrete of both beam and beamstrahlung dumps. Some amount of these neutrons return to the beam tunnel, but most of them are absorbed in the tunnel wall. The rest, about 33,000 neutrons per BX, hit the detector yoke, but few of them reach sub-detectors [8].

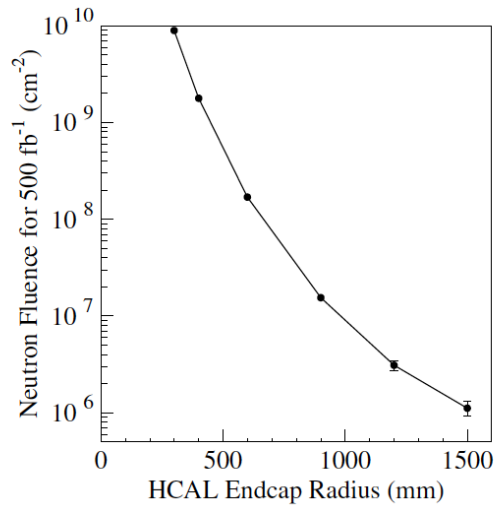


Figure 13. The total neutron fluence at integrated luminosity 500 fb^{-1} in the HCAL endcaps, in dependency of the radial position [9].

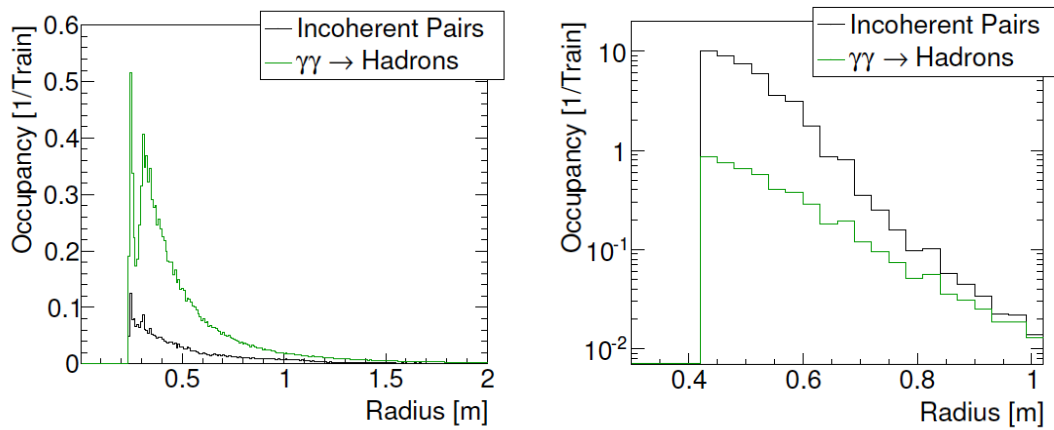


Figure 14. The radial distribution of the train occupancy per pad in ECal (left) and per cell in HCal (right) endcap [10].

References

- [1] A.I. Drozhdin, N.V. Mokhov, N. Nakao, S.I. Striganov, L. Keller, *Suppression of Muon Backgrounds Generated in the ILC Beam Delivery System*, SLAC-PUB-12741 (2007).
- [2] H. Burkhardt, *Background in future linear e^+e^- colliders*, CERN-SL-99-057 AP, CLIC Note 416 (1999).
- [3] D.S. Denisov, N.V. Mokhov, S.I. Striganov, M.A. Kostin, I.S. Tropin, *Machine-Related Backgrounds in the SiD Detector at ILC*, FERMILAB-FN-0790-AD (2006).
- [4] D. Schulte, *Study of Electromagnetic and Hadronic Background in the Interaction Region of the TESLA Collider*, Doctoral thesis, TESLA 1997-08 (1996).
- [5] D. Schulte, *Beam-Beam interaction*, a lecture
www.linearcollider.org/files/ilc_school/Lecture_15_Daniel_Schulte.pdf
- [6] T. Maruyama, *Energy flow comparison between 20 mrad and 2 mrad crossings*, a talk at LCWS2005.
- [7] D. Schulte, *Beam-Beam Simulations with GUINEA-PIG*, CERN-PS-99-014-LP, CLIC-Note-387 (1999).
- [8] G. Wagner, *Neutron Background Studies at TESLA Collider*, LC-DET-2001-148(2001).
- [9] A. Vogel, *Beam-Induced Backgrounds in Detectors at the ILC*, Doctoral thesis, DESY-THESIS-08-036 (2008).
- [10] D. Dannheim and A. Sailer, *Beam-induced Backgrounds in the CLIC Detectors*, LCD-Note-2011-021.